A Theoretical Study on the Mechanism of Oxidation of L-Ascorbic Acid

Yasuo Abe,* Satoshi Okada, Hideo Horii, and Setsuo Taniguchi
Radiation Centre of Osaka Prefecture, Shinke-cho, Sakai 593, Japan
Shinichi Yamabe
Educational Technology Centre, Nara University of Education, Takabatake-cho, Nara 630, Japan

The oxidation of L-ascorbic acid (vitamin C) to dehydroascorbic acid is investigated by *ab initio* MO calculations. Their geometries together with intermediate species are optimized at the STO-3G level. The electron and spin densities are obtained with the 4-31G basis set. The five-membered (γ-lactone) ring is found to be planar during the oxidation process. Neutral and anion radicals are of the similar geometry but are of the different spin-density distribution. The stability of the ascorbate ion and the ascorbate anion radical is attributed to the 'pseudo-aromaticity' involved. The energy variation of the oxidation process of L-ascorbic acid is compared with that of triose reductone which is the simplest molecule having the same functional groups as the former compound.

Ascorbic acid (vitamin C) (AAH_2) plays an important role in various biological processes.[1] AAH_2 is easily oxidized to the product dehydroascorbic acid (DA). During the enzymatic

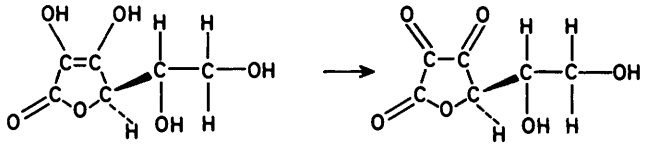

AAH_2 DA

oxidation of AAH_2, transient but stable radicals are formed.[2] The characterization of ascorbate radicals has been carried out by e.s.r.[2,3] The kinetics of their formation and disappearance have also been investigated.[4]

In spite of such extensive studies, the biochemical function of AAH_2 is still not completely understood. To get a deep insight into the oxidation mechanism, information on the electronic structures of AAH_2 and its metabolites is required. Although there is little theoretical work on this subject, reliable data on the electronic structure of these species have not yet been reported. Only the side-chain-free compound, α-hydroxytetronic acid, has been treated with the minimal basis set.[5]

In view of the need for quantitative geometric and electronic structural data, we perform an *ab initio* MO calculation on AAH_2 and its metabolites. To obtain reliable energies, the 4-31G basis set which is of double-zeta quality was adopted. Results for triose reductone (TRH_2) and its oxidized species are also reported. TRH_2 is the simplest molecule with the same functional groups –CO–C(OH)=C(OH)– as AAH_2. TRH_2 is oxidized to dehydroreductone (propanetrione) (DR) in a way similar to $AAH_2 \longrightarrow$ DA.

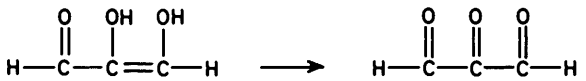

TRH_2 DR

The electronic nature of TRH_2 and DR has been examined previously.[6] The presence or the absence of the five-membered ring and the side chain will change the reactivity of the functional groups. The energetic properties of AAH_2 and TRH_2 have been compared.

Calculations

The electronic structure of L-ascorbic acid (AAH_2), triose reductone (TRH_2), and their metabolites was obtained by *ab initio* MO calculations. Since the molecular size of AAH_2 is large (20 atoms and 92 electrons), the geometry was optimized by the following stepwise procedure.

(1) The geometry of the side-chain-free species was fully optimized, *i.e.* the structure of α-hydroxytetronic acid and its metabolites was determined theoretically without any assumptions.

(2) The geometry of the side-chain group, 1,2-dihydroxyethane, was obtained independently.

(3) To establish the geometry of AAH_2 and its metabolites, partial optimization was carried out. *i.e.* the geometry of α-hydroxytetronic acid was linked to that of the 1,2-dihydroxyethane. The C–C bond distance and the orientation of the side-chain group were optimized.

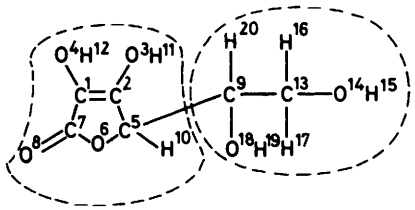

The optimization was made with the STO-3G basis set, followed by one-point calculation with the 4-31G basis set (4-31G//STO-3G). Although STO-3G is small, it reproduces the equilibrium structure. For TRH_2, the full STO-3G optimization and the one-point 4-31G calculation were performed. The planarity of TRH_2 and its metabolites has been confirmed in the previous work by vibrational analysis.[6] All calculations are performed with the GAUSSIAN 80[7] and GAUSSIAN 82[8] programs.

Results and Discussions

In Figure 1, the probable oxidation routes from (**1**) (AAH_2) to (**8**) (DA) are illustrated. In the overall process (**1**) $\longrightarrow$ (**8**), two protons and two electrons are lost. In the neutral solution, the concentration of (**1**) is small, and the ratio of rate constants $k_{(1)\longrightarrow(4)}/k_{(2)\longrightarrow(5)}$ is only 0.01.[9] Therefore, the cation radical (**4**) plays a minor role and is not considered here.

AAH^- (**2**) is a conjugate base of (**1**) and is in equilibrium with

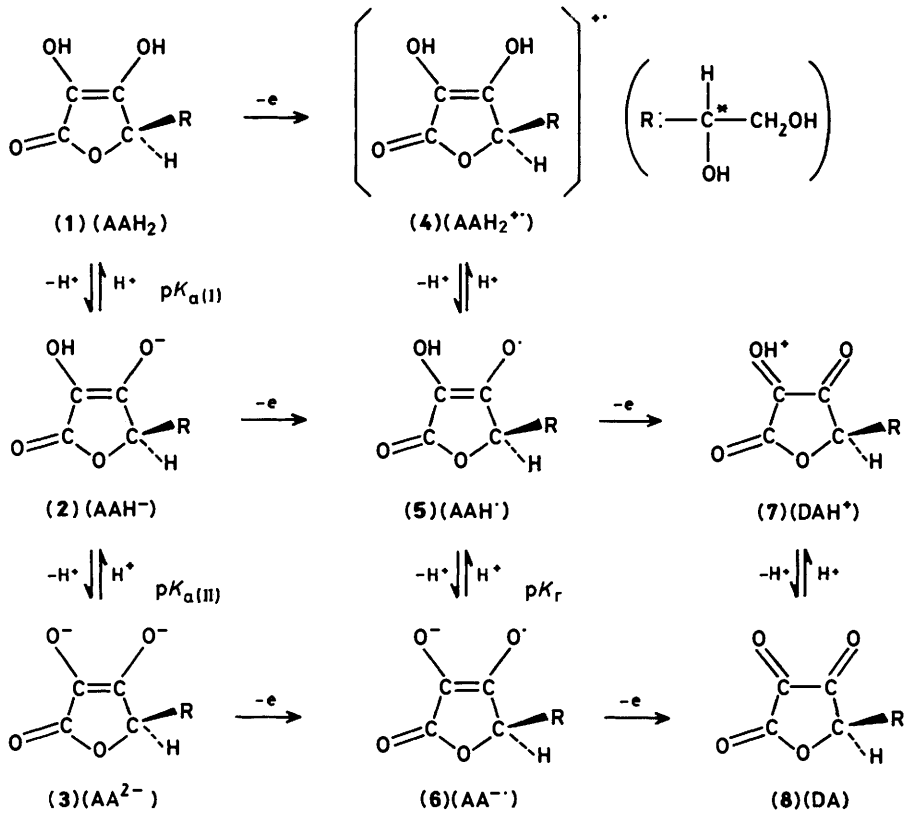

Figure 1. Probable oxidation routes from L-ascorbic acid (AAH_2) to dehydroascorbic acid (DA)

Table 1. Comparison of physical properties of triose reductone (TRH_2) and L-ascorbic acid (AAH_2)

Properties	Triose reductone			L-Ascorbic acid		
Molecular formula	$C_3H_4O_3$			$C_6H_8O_6$		
Molecular weight	88			176		
M.p. (°C)	161[a]			190—192[b]		
pK_a	(I) 5.03, (II) 13.0[c]			(I) 4.17, (II) 11.57[d]		
pK_r	1.4[e]			−0.45[f]		
U.v. spectra	$\lambda_{max.}$/nm[c]	ε	pH	$\lambda_{max.}$/nm[g]	ε	pH
	268	16 300	3.8	245	12 200	2.0
	293	24 600	8.0	265	16 500	6.4
	323	23 300	13.5			

[a] Ref. 12. [b] Ref. 13. [c] Ref. 10. [d] Ref. 14. [e] Ref. 15. [f] Ref. 3. [g] Ref. 16.

it, $pK_{a(I)}$. Species (**3**) is the dianion AA^{2-} which is also in equilibrium, $pK_{a(II)}$, with (**2**). The neutral radical (**5**) and the anion radical (**6**) are in a different equilibrium, pK_r. The judgement of which route is most probable is of central interest and is described later. The oxidation mechanism of AAH_2 is similar to that of TRH_2. The oxidation of TRH^- by O_2 is 40 times faster than that of AAH^-.[10,11] The difference lies in the stability of products, DA and DR. DA may be isolated as a dimer, and it is stable as a hydrated compound in aqueous solution. On the other hand, DR is oxidized to give formic acid, which means the reverse reaction (DR ⟶ TRH_2) is unlikely.

In Table 1, some observed physical properties of AAH_2 and TRH_2 are displayed. The difference in pK_a and pK_r between the two species is noticeable. There should be some differences in their electronic nature.

Optimized Geometries of L-*Ascorbic Acid and its Metabolites.*—In Figure 2, the optimized geometry of AAH_2 is shown together with that of TRH_2 (**1′**). Geometric parameters obtained here agree with *X*-ray data.[17] The five-membered ring is calculated to be almost planar. The puckering angle is only 0.3°. Metabolites (**2**)—(**8**) are also planar species. The functional group of AAH_2 has a geometry similar to that of TRH_2.

In Figure 3, the structures of the iso-electronic species (**2**) and (**3**) are shown. By the first deprotonation [(**1**) ⟶ (**2**)], a hydroxy

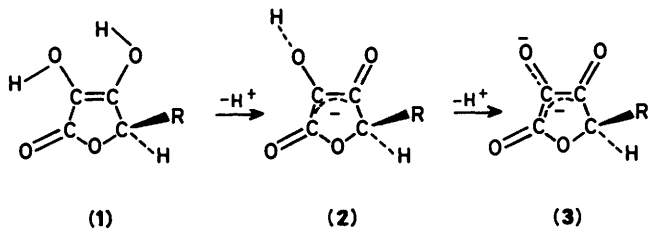

(**1**) (**2**) (**3**)

Scheme 1.

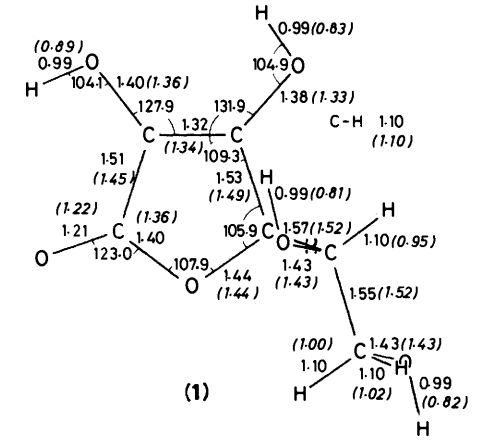

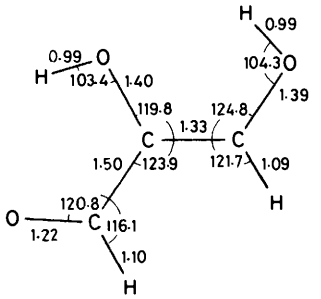

Figure 2. The optimized geometry of AAH_2 (**1**) and TRH_2 (**1'**). Values in italics in parentheses are *X*-ray experimental data from ref. 17. Bond lengths are in Å and angles in degrees

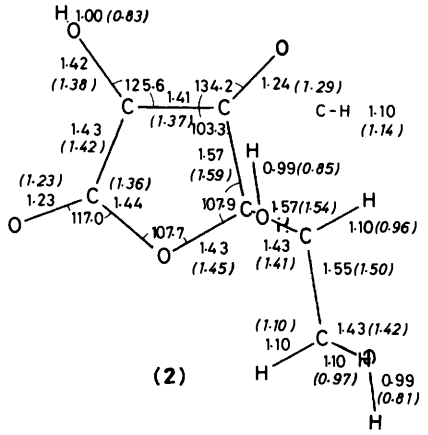

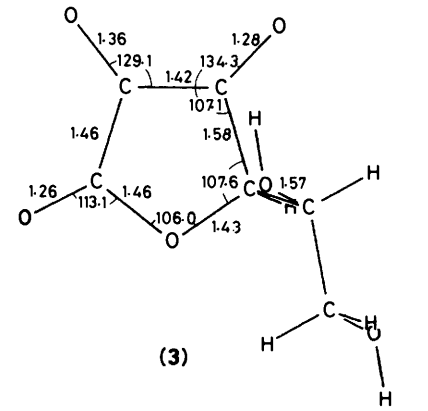

Figure 3. Optimized geometries of AAH^- (**2**) and AA^{2-} (**3**). For (**2**), *X*-ray data are also exhibited [18]

group is converted into a carbonyl group. On the second deprotonation, however, such a distinct bond conversion is not observed. Species (**2**) is already a '6π electron' system (the π electronic charge is 6.138), and the five-membered ring rejects the invasion of the extra π electron in (**3**).

In Figure 4, geometries of the iso two electronic species (**5**) and (**6**) are exhibited. The intermediacy of neutral and anion radicals is clearly demonstrated. Upon oxidation, (**2**) ⟶ (**5**) or (**3**) ⟶ (**6**), the geometry is not changed significantly. The calculated atomic spin densities ρ are also shown in Figure 4. There has been much unresolved discussion [3,5] of this property. Our results are represented in Scheme 2.

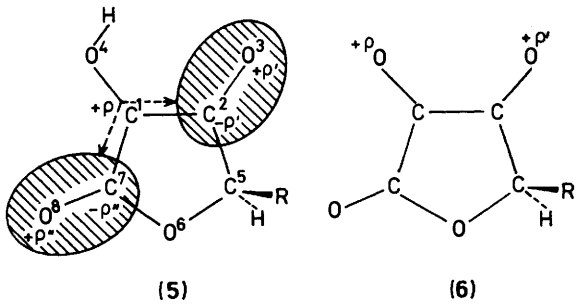

Scheme 2.

In (**5**), the radical centre is C(1), and the spin density causes *spin polarization* of two carbonyl groups. In (**6**), the densities are outside the five-membered ring and are on the two oxygen atoms O(3) and O(4). The densities of (**6**) are not so delocalized as those of (**5**). This difference is interpretable in terms of that of the electron distribution in the two precursors (**2**) and (**3**) in Scheme 1.

In Figure 5, structures of the isoelectronic species (**7**) and (**8**) are shown. By a second electron loss, (**5**) ⟶ (**7**), a hydroxy group is converted into the protonated carbonyl group. In (**7**) and (**8**), there are two single C–C bonds and three carbonyl groups. In contrast, in (**5**) and (**6**), the position is not clear due to π-electron delocalization. The reactivity of (**8**) towards nucleophilic attack is of mechanistic interest. (i) Among the three carbonyl groups, which is hydrolysed most readily? (ii) How is the five-membered ring of (**8**) opened? These two questions may be answered by the frontier-electron theory. [19]

(i) In the LUMO of (**8**), the largest spatial extension is for C(1)=O(4). Therefore, it is most probable that a water molecule

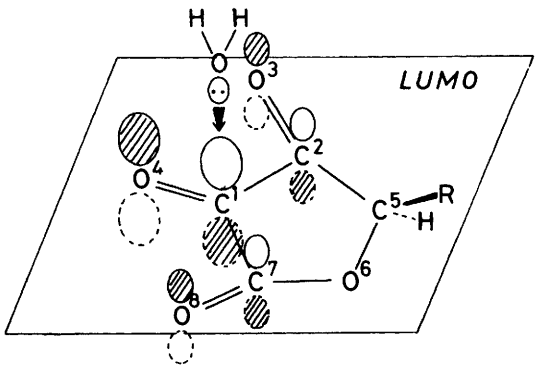

Scheme 3.

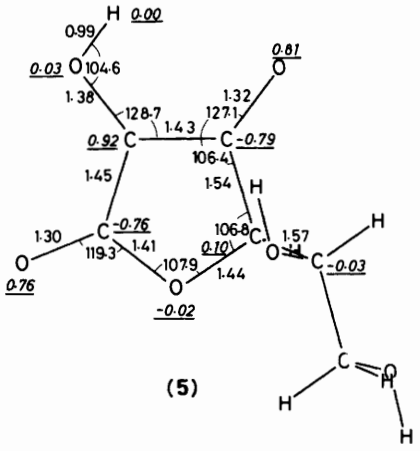

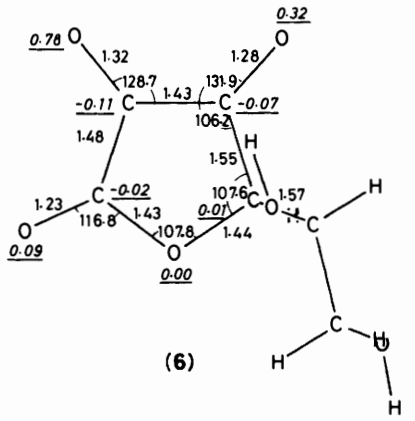

Figure 4. Optimized geometries of $AAH^{\cdot}$ (**5**) and $AA^{-\cdot}$ (**6**). Italics denote the atomic spin densities (ρ) evaluated by the UHF of the 4-31G basis set

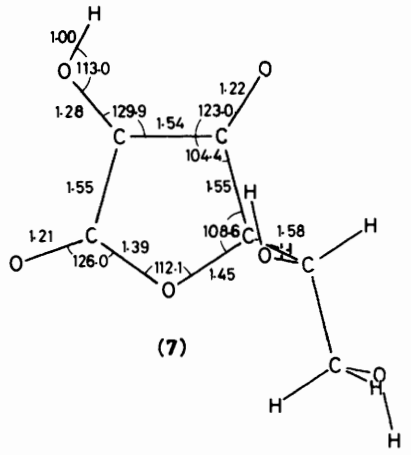

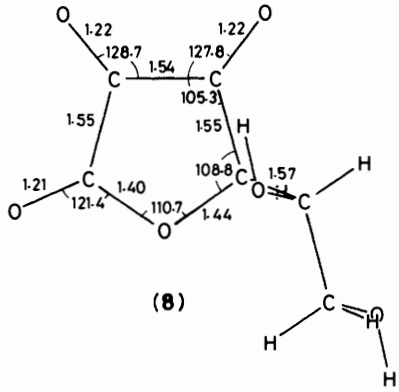

Figure 5. Optimized geometries of DAH^{+} (**7**) and DA (**8**)

approaches it. This prediction is supported by experimental evidence.[20] (ii) The in-plane low-lying vacant MO of (**8**) is the

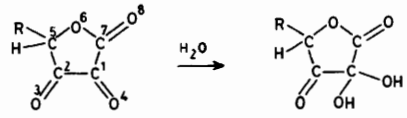

third LUMO, (LU + 3)MO. A σ*-type MO preferentially accepts electron density from the nucleophile X^{-}. Charge

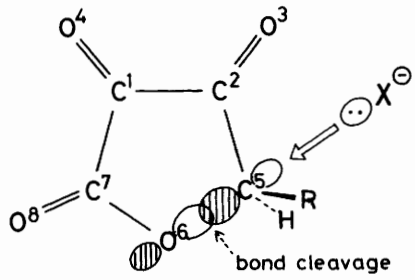

Scheme 4.

transfer leads naturally to the C(5)–O(6) bond scission due to the strong C(5)–O(6) antibonding character of (LU + 3)MO. In fact, conversion of (**8**) into a branched acid in neutral and alkaline aqueous solution has been reported.[21] Thus, the

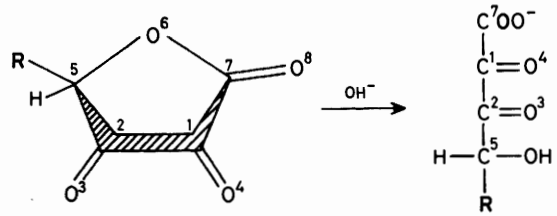

(**8**)

conversion of (**8**) into an open-chain product is defined as an S_N2 reaction.

The deprotonation (**1**) ⟶ (**2**) gives delocalization of the π-electrons in the five-membered ring. That is, proton loss from (**1**) leads to increased energy of the π MOs and the subsequent greater power of reduction. The second deprotonation (**2**) ⟶ (**3**) is not so facile as (**1**) ⟶ (**2**), because the dianion AA^{2-} is thermodynamically unstable. The first π electron loss, (**2**) ⟶ (**5**) or (**3**) ⟶ (**6**), gives rise to a stable ascorbate radical. For the second oxidation, the odd π electron may be removed readily from radical (**5**) or (**6**) to give the triketone system (**7**) or (**8**). During the overall process, the planarity of the five-membered ring is maintained. Deprotonation occurs through the hydrogen bond with a water molecule in the plane. It raises the energy levels of the π orbitals, leading to easier oxidation. Thus, in-plane deprotonation enhances out-of-plane electron loss effectively. All species are found to have equilibrium geometries.

Table 2. Total energy E_T and energies of frontier orbitals calculated with the 4-31G basis set

Oxidation of triose reductone						Oxidation of L-ascorbic acid					
No.	Compound	E_T (a.u.)	HOMO (a.u.)	LUMO (a.u.)	SOMO (a.u.)	No.	Compound	E_T (a.u.)	HOMO (a.u.)	LUMO (a.u.)	SOMO (a.u.)
(1′)	TRH_2	−339.970 34	−0.359 29	0.077 43		(1)	AAH_2	−679.977 08	−0.377 07	0.091 93	
(2′)	TRH^-	−339.418 43	−0.099 13	0.300 85		(2)	AAH^-	−679.443 70	−0.144 51	0.298 78	
(3′)	TR^{2-}	−338.620 05	0.159 22	0.492 70		(3)	AA^{2-}	−678.679 33	0.118 41	0.403 18	
(5′)	$TRH^{\cdot}$	−339.389 04		0.088 26	−0.406 28	(5)	$AAH^{\cdot}$	−679.376 10		0.091 52	−0.423 29
(6′)	$TR^{-\cdot}$	−338.839 53		0.275 94	−0.121 76	(6)	$AA^{-\cdot}$	−678.870 06		0.269 50	−0.150 23
(7′)	DRH^+	−339.047 67	−0.696 13	−0.269 06		(7)	DAH^+	−679.034 93	−0.581 51	−0.279 76	
(8′)	DR	−338.781 88	−0.431 67	−0.003 50		(8)	DA	−678.784 81	−0.436 85	−0.027 39	

1 a.u. = 1 hartree = 627.566 kcal mol^{-1}; HOMO is the highest occupied MO; LUMO is the lowest unoccupied MO; SOMO is the singly occupied MO.

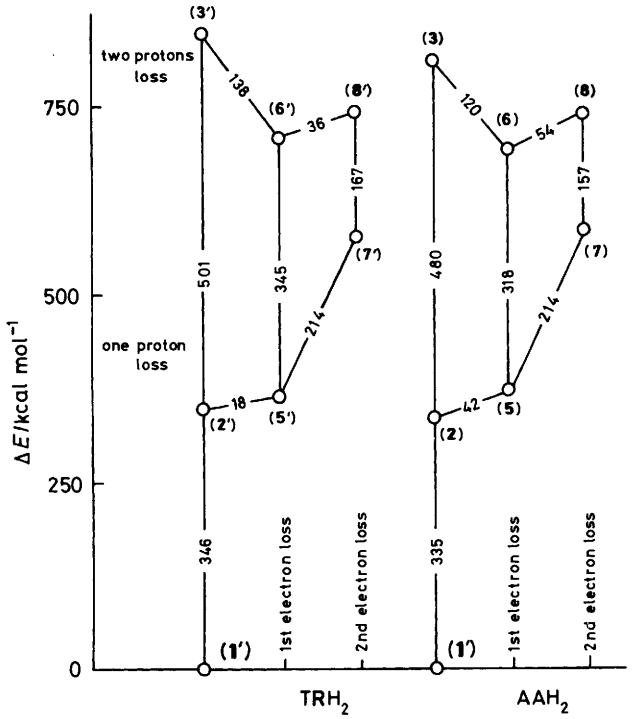

Figure 6. The 4-31G energy variations for proton and electron removal, (1′) ⟶ (8′) and (1) ⟶ (8) in kcal mol^{-1}

Energy Comparison between TRH_2 *and* AAH_2.—In Table 2, the total and orbital energies of TRH_2, AAH_2, and their metabolites are displayed. The change of total energies along the oxidation route in Figure 1 is drawn in Figure 6. In Figure 6, proton loss causes significant destabilization. The MO calculation deals with the naked ion in the gas phase. In solution, however, destabilization is cancelled out by stronger solvation (hydration) stabilization. In aqueous media, therefore, the energies of all species are comparable. Since the solvent effect on oxidation is thought to be of the same magnitude, a comparison of two energy changes is meaningful. There is a noticeable difference in the energy gap between (1′) and (2′) (346) and (1) and (2) (335 kcal mol^{-1}). This means that AAH_2 undergoes the first deprotonation more readily than TRH_2. The $pK_{a(I)}$ values in Table 1 reflect this trend. The difference of energy gap for (2′)—(3′) (501) and (2)—(3) (480 kcal mol^{-1}) is larger, which is in accord with that of the $pK_{a(II)}$ values in Table 1. The anion AA^{2-} is more likely to be formed than TR^{2-}. The ease of deprotonation from AAH_2 or AAH^- relative to that of TRH_2 or TR^- is ascribed to the stability of the conjugate base, AAH^- or AA^{2-}. $pK_{a(I)} < pK_{a(II)}$ in Table 1 is reflected by the difference of energy gaps, (1)—(2) and (2)—(3). It is noteworthy that the first electron loss (2) ⟶ (5) is more difficult than (2′) ⟶ (5′). The stable anion (2) with 6π electrons resists electron loss. The second proton loss (5) ⟶ (6) is more likely than (5′) ⟶ (6′). Again, the stability of the 6π-electron system is increased in (6). The difference in the values of pK_r in Table 1 (1.4 *versus* −0.45) is consistent with that of the energy gaps. The energy increases by 214 kcal mol^{-1} for the second electron loss [(5) ⟶ (7) and (5′) ⟶ (7′) are fortuitously the same]. The route (6) ⟶ (8) is more difficult than (6′) ⟶ (8′). The stability ('pseudo-aromaticity') of (6) resists electron loss. This is similar to the (2) ⟶ (5) route. Thus, the major oxidation route of AAH_2 is different from that of TRH_2. Roughly speaking, TRH_2 takes the (1′) ⟶ (2′) ⟶ (5′) ⟶ (7′) ⟶ (8′) route. In contrast, AAH_2 prefers the (1) ⟶ (2) ⟶ (5) ⟶ (6) ⟶ (8) and (1) ⟶ (2) ⟶ (3) ⟶ (6) ⟶ (8) routes.

Conclusions.—In this work, geometries of L-ascorbic acid and its metabolites are determined theoretically. The five-membered ring is found to be planar throughout the oxidation process. This is needed to release two π electrons readily. Deprotonation enhances this π electron release and converts the hydroxy into the carbonyl group. The energy changes along various routes are compared between AAH_2 and TRH_2. The combination of the ene-diol group and the γ-lactone ring in AAH_2 gives a reactivity different from that of the ene-diol and a carbonyl in TRH_2. In particular, the intermediate species (2) and (6) are stable relative to (2′) and (6′). This is due to the 'pseudo-aromaticity' involved in the former molecules. The radical intermediates 5 and 6 are found to have similar geometries but different spin-density distributions. The side-chain alkyl group has a small effect on the energy change of AAH_2 of Figure 6. There is a 10 kcal mol^{-1} difference (at most) in the energy gap between AAH_2 and α-hydroxytetronic acid. It is confirmed that AAH_2, with the ene-diol and γ-lactone, is suitable for both ready π electron release and stability of intermediates.

Acknowledgements

We thank the Data Processing Centre of Kyoto University for allotment of CPU time at the FACOM M-382 computer. Thanks are also due to the Institute for Molecular Science for use of the HITAC M-200H computer.

References

1 'Ascorbic Acid: Chemistry, Metabolism, and Uses,' eds. P. A. Seib and B. M. Tolbert, Am. Chem. Soc. Adv. in Chem. Ser. No. 200, Washington, 1982.

2 I. Yamazaki, H. S. Mason, and L. H. Piette, *J. Biol. Chem.*, 1960, **235**, 2444.
3 G. P. Laroff, R. W. Fessenden, and R. H. Schuler, *J. Am. Chem. Soc.*, 1972, **94**, 9062.
4 B. H. J. Bielski, A. O. Allen, and H. A. Schwarz, *J. Am. Chem. Soc.*, 1981, **103**, 3516.
5 C. Thomson, *J. Mol. Struct.*, 1980, **67**, 133; P. R. Laurence and C. Thomson, *Int. J. Quantum. Chem., Quantum Biol. Symp.*, 1981, **8**, 81.
6 Y. Abe, H. Horii, S. Taniguchi, S. Yamabe, and T. Minato, *Can. J. Chem.*, 1986, **64**, 366.
7 J. S. Binkley, R. A. Whiteside, R. Krishnan, R. Seeger, D. J. DeFrees, H. B. Schlegel, S. Topiol, L. R. Kahn, and J. A. Pople, *QCPE*, 1981, **13**, 406.
8 J. S. Binkley, R. A. Whiteside, K. Raghavachari, R. Seeger, D. J. DeFrees, H. B. Schlegel, M. J. Frisch, J. A. Pople, and L. R. Kahn, 'Gaussian 82 Release A,' Carnegie-Mellon University, Pittsburg, 1982.
9 M. Kimura, M. Yamamoto, and S. Yamabe, *J. Chem. Soc., Dalton Trans.*, 1982, 423.
10 Y. Abe, H. Horii, S. Taniguchi, K. Kamai, and M. Takagi, *Bull. Chem. Soc. Jpn.*, 1983, **56**, 467.
11 A. Weissberger, J. E. LuValle, and D. S. Thomas, Jr., *J. Am. Chem. Soc.*, 1943, **65**, 1934.
12 H. v. Euler and C. Martius, *Justus Liebigs Ann. Chem.*, 1933, **505**, 73.
13 J. C. Bauernfeind, ref. 1, p. 397.
14 T. W. Birch and L. J. Harris, *Biochem. J.*, 1933, **27**, 595.
15 H. Horii, Y. Abe, and S. Taniguchi, *Bull. Chem. Soc. Jpn.*, 1985, **58**, 2751.
16 J. S. Lawendel, *Nature* (*London*), 1957, **180**, 434.
17 J. Hvoslef, *Acta Crystallogr., Sect. B*, 1968, **24**, 23.
18 J. Hvoslef, *Acta Crystallogr., Sect. B*, 1969, **25**, 2214.
19 K. Fukui, 'Theory of Orientation and Stereoselection,' Springer Verlag, Berlin, 1970.
20 B. M. Tolbert and J. B. Ward, ref. 1, pp. 113—116.
21 L. Lowendahl and G. Petersson, *Anal. Biochem.*, 1976, **72**, 623.

Received 28*th April* 1986; *Paper* 6/804